Mem. S.A.It. Suppl. Vol. 20, 15

Memorie della
Supplementi

Photometric Analysis of Asteroid (2867) Steins from Rosetta OSIRIS Images

F. La Forgia[1], S. Magrin[1], I. Bertini[1,2], M. Lazzarin[1], M. Pajola[1,2] and C. Barbieri[1,2]

[1] Department of Astronomy – University of Padova, vicolo dell'Osservatorio 3, 35122 Padova, Italy
[2] CISAS "G. Colombo" – University of Padova, via Venezia 15, 35131, Padova, Italy

e-mail: fiorangela.laforgia@studenti.unipd.it

Abstract. We present a method for analyzing the reflectance properties of atmosphereless bodies as asteroids and comet nuclei. The method is self-consistent, independent of the shape model of the object and can be easily applied for any space mission target. We used it for the E-type Main Belt asteroid (2867) Steins, observed from the OSIRIS–WAC camera onboard Rosetta spacecraft during a close approach on September 5, 2008.
We investigate the reflectance dependence on phase angle which is interpreted in terms of the Hapke's theory of bidirectional reflectance.
A deeper analysis allows to obtain an estimate of the typical size of the regolith grains.
Steins regolith layer seems to be made of large, highly scattering iron-poor opaque silicate particles. The macroscopic roughness, probably influenced by the global irregular shape, appears fairly high, comparable with radar measurements of other E-type asteroids. Assuming an enstatite composition, we estimated a grain size of about 30–130 μm and we noticed a correlation between grain size and wavelength, suggesting the existence of a grain size distribution, as expected from real surfaces.
The comparison with more accurate calculations (Spjuth *et al.*, 2009) shows that our simplified method is robust and reliable for a preliminary and shape-independent analysis of the reflectance properties of atmosphereless bodies.

Key words. Asteroids – Photometry – Phase curve – Regolith – Grain size

1. Introduction

Many space missions today are dedicated to small bodies of the Solar System, as asteroids and comets, samples of the primordial planetesimals that accreted in the solar nebula. They are key bodies for understanding the dynamical, chemical and physical processes occurred during the initial phases of the formation of the Solar System.
Each asteroid is a world of its own because of the different origin and history. Asteroids show a wide range of masses and diameters, from few centimeters up to 1000 km, great diversity of superficial composition, features (rough/smooth terrains, craters, hills, depressions), optical properties, and dynamical be-

haviors.

The European Space Agency mission Rosetta was launched on March 2, 2004 to its final target, the comet 67P/Churyumov–Gerasimenko. Rosetta's main objective is to rendez-vous with the comet and enter orbit around it performing observations of the comet's nucleus and coma and measuring its activity increase as the comet approaches its perihelion. During the long trek towards the comet, the spacecraft performed two fly–bys with secondary targets: the E-type 6-km Main Belt asteroid (2867) Steins on September 5, 2008 (Keller *et al.*, 2010) and the asteroid 21 Lutetia on July 10, 2010 (Sierks *et al.*, 2011). During the Steins fly–by, the Wide Angle Camera (WAC) of the Optical Spectroscopic and Infrared Imaging System (OSIRIS) onboard Rosetta was deeply operating and obtained high resolution images of Steins surface up to 80 m/px from a minimum distance of 803 km.

2. Method

The considered data set comprises 349 WAC images taken in 12 different filters in the wavelength range [250,1000] nm covering approximately 60% of the surface of Steins. Images were previously reduced and calibrated by subtraction of bias, normalization to exposure time, removal of bad pixels, division by flat field and conversion to radiometric units.

For the photometric analysis we use a limb determination to select the asteroid area in order to avoid spurious light due to straylight from brigth out-of-axis sources in the field of view, ghosts and cosmic rays. We then investigate, for each filter, the reflectance dependence on the phase angle, which is interpreted in terms of the Hapke's bidirectional reflectance theory (Hapke, 1993). Five parameters are measured describing the optical properties of the regolith layer covering the asteroid and responsible for the light scattering. A deeper analysis of the single scattering albedo, one of the Hapke's parameters, allows to obtain an estimate of the typical size of the regolith grains with an appropriate assumption on the composition.

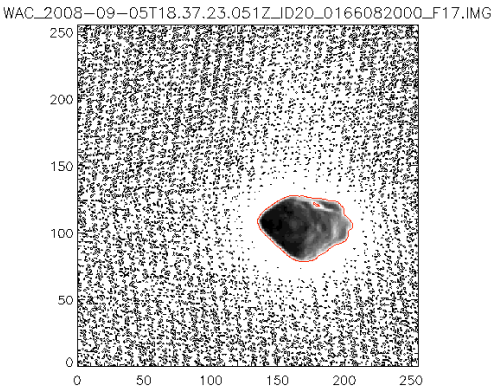

Fig. 1. CA image of (2867) Steins with selected contour defined using a threshold level on the flux that maximizes the S/N.

2.1. Limb determination

The limb determination, i.e. the selection of the contour that enclose the region of interest from the background, is done using the criterion of maximizing the signal to noise ratio (S/N). The contour is defined using a threshold level of minimum flux. The higher the threshold, the smaller the area selected by the contour around the asteroid. The selected threshold is the one that defines the contour that maximizes the S/N inside itself. The image obtained at the closest approach (CA) between the spacecraft and the asteroid is shown in Fig. 1 and the selected contour is overplotted (red curve). The S/N as function of the threshold level for the same image is shown in Fig. 2.

2.2. Reflectance measurement

Once the region of interest is selected for each image, the disk-averaged reflectance is measured. The reflectance is the fraction of incident light scattered or reflected by a surface. It depends on the geometry of illumination and observation and on the physical and chemical characteristics of the surface material. Steins reflectance r can be calculated as:

$$r(\alpha) = \frac{\pi \cdot F_S(\alpha)}{F_\odot} \quad (1)$$

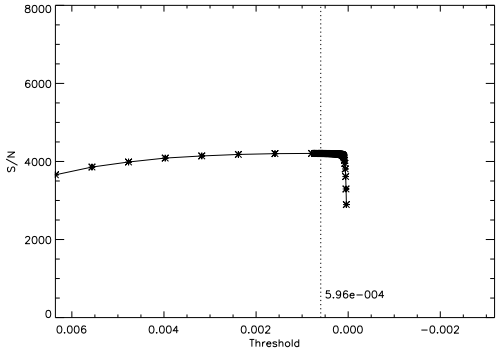

Fig. 2. S/N as function of different threshold levels. The maximum value selects the asteroid limb shown in Fig. 1.

Table 1. WAC filters.

filter name	filter code	central wavelength [nm]	bandwidth [nm]
OI	17	631.60	4.0
Na	16	590.70	4.7
NH_2	15	572.10	11.5
CN	14	388.40	5.2
UV375	13	375.60	9.8
NH	81	335.90	4.1
UV325	71	325.80	10.7
OH	61	309.70	4.1
UV295	51	295.90	10.9

where α is the phase angle, defined as the angle between the light incident onto the object and the light reflected by the object. In our case α is the smallest of the angles Sun-Steins-Rosetta. F_S is the flux observed (also called brightness, radiance, or specific intensity) by a surface element of the detector in a unit solid angle per unit wavelength and it is expressed in W m^{-2} nm^{-1} sr^{-1}. In our case F_S is evaluated using the median of the pixel values in the selected area. $F_\odot$ is the solar spectral irradiance, the solar flux incident on a surface element of the target per unit wavelength expressed in W m^{-2} nm^{-1}. In our case it is the solar flux observed through the same filter as Steins at its heliocentric distance.

2.3. Phase curve

As the flux F_S depends on α, the reflectance r depends also on α. The function $r(\alpha)$ describes the phase curve. Steins phase curve is shown in Fig. 3 for all available WAC filters summarized in Table 1.

During the fly-by the phase angle was rapidly changing from the initial value of about $-38°$ to a minimum value of $0.36°$ to increase again to the maximum value of $136°$.

2.4. Hapke's model

Hapke's theory of bidirectional reflectance (Hapke, 1993) allows to solve the inverse scattering problem for a planetary surface. Starting from the phase curve of the surface we use this model to achieve information on the physical and mineralogic properties of the regolith surface and the grains composing it. Modeling the phase curve with a multiparametric function we measure in total five parameters: the single scattering albedo, w, the asymmetry factor of the single particle phase function, g, the magnitude of the opposition effect, B_0, the angular width of the opposition effect, h, and the macroscopic roughness, θ.

The single scattering albedo is the fraction of the total amount of incident light scattered by a single spherical particle. It contains information on the reflectance of the single particles forming the regolith, therefore it gives hints on its mineralogical composition.

The single particle phase function describes the pattern of the scattered light as function of the phase angle for a single particle. If the particle does not scatter isotropically this function is asymmetric and g described this property. It contains information about the optical behavior of the particle and therefore its dimension. If the particle is small enough indeed, it mainly diffracts the light, otherwise it behaves as in usual geometrical optics.

The opposition effect is a non-linear increase in brightness as the phase angle approaches zero, occurring in all porous, particulate media. In Fig. 4 it is shown the astronaut's shadow projected on the Moon's surface. The phase angle is about zero in the center of the image and increases towards the boulders. The in-

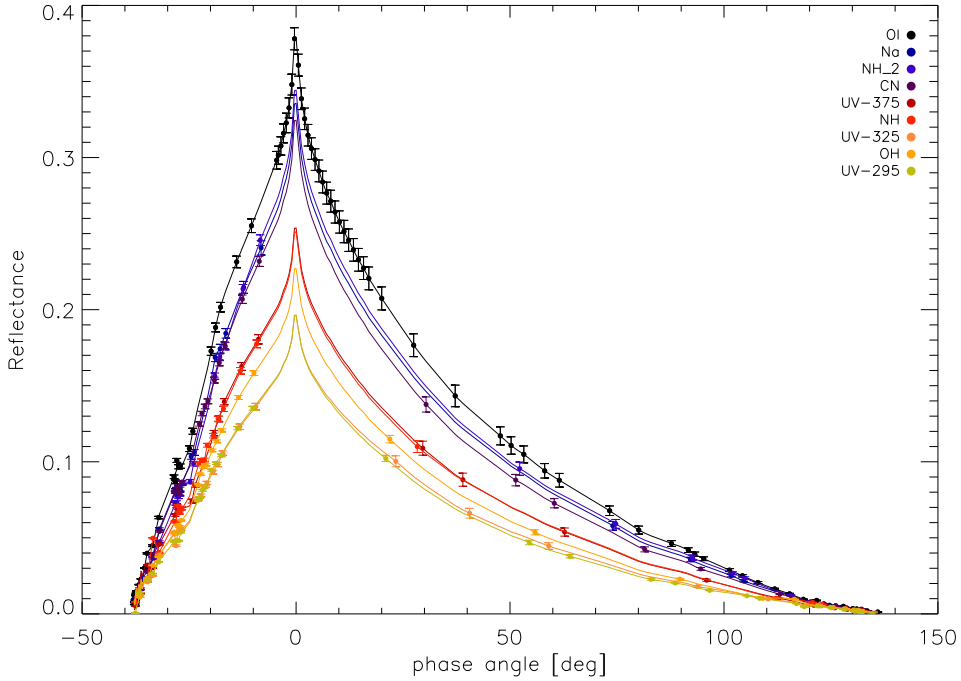

Fig. 3. Phase curve in all available OSIRIS-WAC filters. OI filter phase curve has been interpolated and the peak value scaled for all the other filters.

Table 2. Hapke's parameters and χ^2 for all available WAC filters.

wavelength	filter	w	g	B_0	h	θ	χ^2
631.60	17	0.609 ± 0.015	-0.294 ± 0.010	0.712 ± 0.051	0.030 ± 0.003	26.4 ± 5.3	0.0011
590.70	16	0.558 ± 0.012	-0.282 ± 0.007	0.729 ± 0.043	0.038 ± 0.003	25.8 ± 3.9	0.0014
572.10	15	0.572 ± 0.012	-0.277 ± 0.007	0.751 ± 0.044	0.039 ± 0.003	24.7 ± 3.9	0.0014
388.40	14	0.525 ± 0.014	-0.303 ± 0.008	0.668 ± 0.049	0.038 ± 0.004	26.1 ± 4.4	0.0019
375.60	13	0.421 ± 0.012	-0.316 ± 0.008	0.603 ± 0.045	0.034 ± 0.004	27.1 ± 4.3	0.0013
335.90	81	0.474 ± 0.014	-0.286 ± 0.013	0.531 ± 0.048	0.035 ± 0.005	39.1 ± 3.1	0.0017
325.80	71	0.339 ± 0.007	-0.299 ± 0.005	0.670 ± 0.034	0.036 ± 0.003	20.5 ± 3.9	0.0004
309.70	61	0.347 ± 0.002	-0.276 ± 0.004	1.000 ± 0.000	0.063 ± 0.003	7.9 ± 3.4	0.0017
295.90	51	0.307 ± 0.018	-0.272 ± 0.003	0.994 ± 0.119	0.064 ± 0.005	8.0 ± 17.4	0.0010

creased brightness in this region is clearly visible and it is further emphasized by the reduced brightness of the shadow, resulting in an halo around the head of the astronaut. This is why the opposition effect is called *heiligenschein*, that means literally saint's shine. This phenomenon is primarily caused by the fact that at zero phase angle each particle hides its own shadow (shadow hiding) and thus the surface appears brighter. Fig. 5 shows such effect at decreasing resolution. B_0 parameter describes mainly the amplitude of the opposition effect while h describes its angular width. B_0 in particular is related with the opacity of the particles that tunes the ability to hide their own shadows. Opaque particles show a high values

Fig. 4. Representation of the opposition effect. Astronaut's shadow on the Moon's surface. The phase angle is zero in the center of the image, thus the opposition effect results in a bright halo around the astronaut's head.

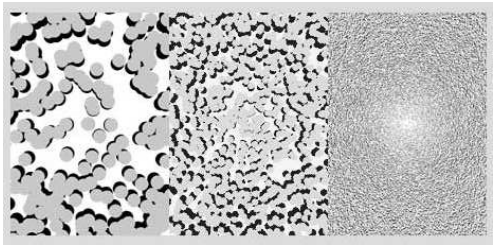

Fig. 5. Particles hiding its own shadow. Phase angle is zero at the center of each panel of the image. Resolution decreases from the left panel to the right one.

of B_0, while transparent grains have a reduced ability to hide the shadows.
The last parameter θ describes the macroscopic roughness of the surface that influences the reflectance as it changes the geometry of the event. It may be influenced also by the global shape of the object.

We perform an iterative Levenberg-Marquardt least-squares fit (Levenberg, 1944 & Marquardt, 1963) of Steins phase curve with the theoretical Hapke's function in all available WAC filters obtaining the five parameters described above. The resulting fit in the OI filter is shown in Fig. 6 (red line) and the resulting values of Hapke's parameters for all filters are reported in Table 2.

2.5. Grain size estimate

Using the Hapke's model it is possible to derive analytic approximations for the scattering efficiency of an isolated spherical particle as a function of its size, if an appropriate composition is assumed. Moreover, an exact solution of Maxwell's equations describing the scattering problem can be found for these particles using the Mie theory (Mie, 1908 & Hansen, 2009). For a given composition, direct relations exist between the single scattering albedo and the diameter of the particle D, $w(D)$, depending on the method used (e.g. slab approximation, slab exact (Hapke, 1993) and Mie-δ Eddington (Joseph *et al.*, 1976)). Comparing the value of the w obtained during the fitting procedure with different theoretical $w(D)$ relationships, it is possible to infer a gross estimate of the grain size range forming the regolith.

The spectral type and the mineralogical studies suggest that Steins is coated by enstatite or similar iron-poor silicates (Barucci *et al.*, 2008). Exposition to space environment indicates that enstatite is probably present in its amorphous form (Jäger *et al.*, 2003). Using this composition we derived the analytical expressions of $w(D)$ and compared them to the fitted value for all available WAC filters. In Table 3 are reported the values obtained while in Fig. 7 is shown the comparison for the OI filter.

3. Results

Fitting the disk-averaged phase curve of Steins we obtained wavelength-dependent Hapke's parameters (Table 2). The fitted single scattering albedos have high values, consistent with a bright body, as expected for an E-type asteroid. The asymmetry factor of the single particle phase function shows a negative value for all filters. This suggests that particles are mainly backscattering indicating that the regolith is probably dominated by particles much larger than the observational wavelengths. A negative value of the asymmetry factor also suggests the

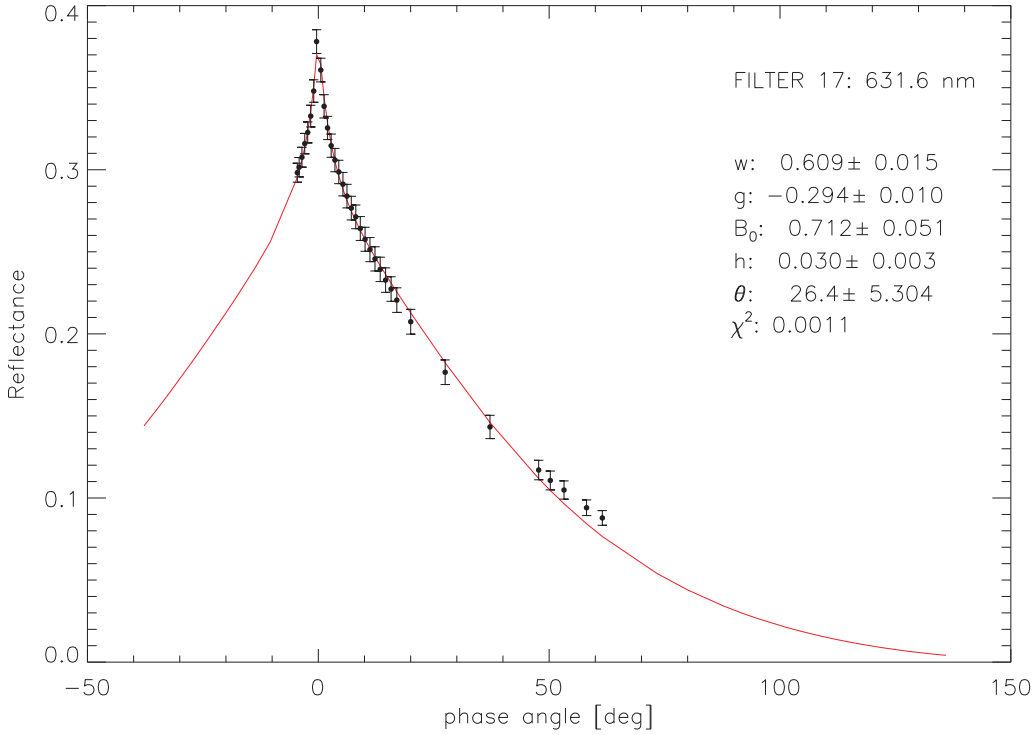

Fig. 6. Steins phase curve fitted with theoretical Hapke's bidirectional reflectance multiparametric function.

Table 3. Grain size estimate for different filters.

wavelength [nm]	filter	w	grain size [μm] min	max
631.60	17	0.609 ± 0.015	80	130
590.70	16	0.558 ± 0.012	90	130
572.10	15	0.570 ± 0.012	80	120
388.40	14	0.552 ± 0.016	30	50
375.60	13	0.421 ± 0.012	50	80
335.90	81	0.428 ± 0.007	30	50
325.80	71	0.366 ± 0.003	40	60
309.70	61	0.397 ± 0.005	30	50
295.90	51	0.350 ± 0.055	30	50

presence of irregular-shaped particles that contain more reflective inclusions. The opposition effect amplitude shows moderately to high values. This suggests that the surface of Steins consists of opaque silicate particles with little or no iron component. The angular width parameter shows a narrow opposition effect. The macroscopic roughness seems to be fairly high. This result is consistent with radar observations performed by Benner *et al.* (2008) who found an enhanced surface roughness for E-type asteroids.

Grain size estimate is essential to understand the space weathering process at which the asteroid is exposed during its all life. Assuming that Steins surface is made of amorphous enstatite grains, we found a grain size in the range [30-130] μm. This is consistent with the negative value of g, suggesting ∼100-μm sized particles. The comparison with Li *et al.* (2004) who measured Hapke's parameters for different mixtures of silicates, confirms the assumption of silicate composition. We found a slight grain diameter dependence on wavelength suggesting that there is a grain size distribution on Steins superficial regolith layer, as expected for a realistic material.

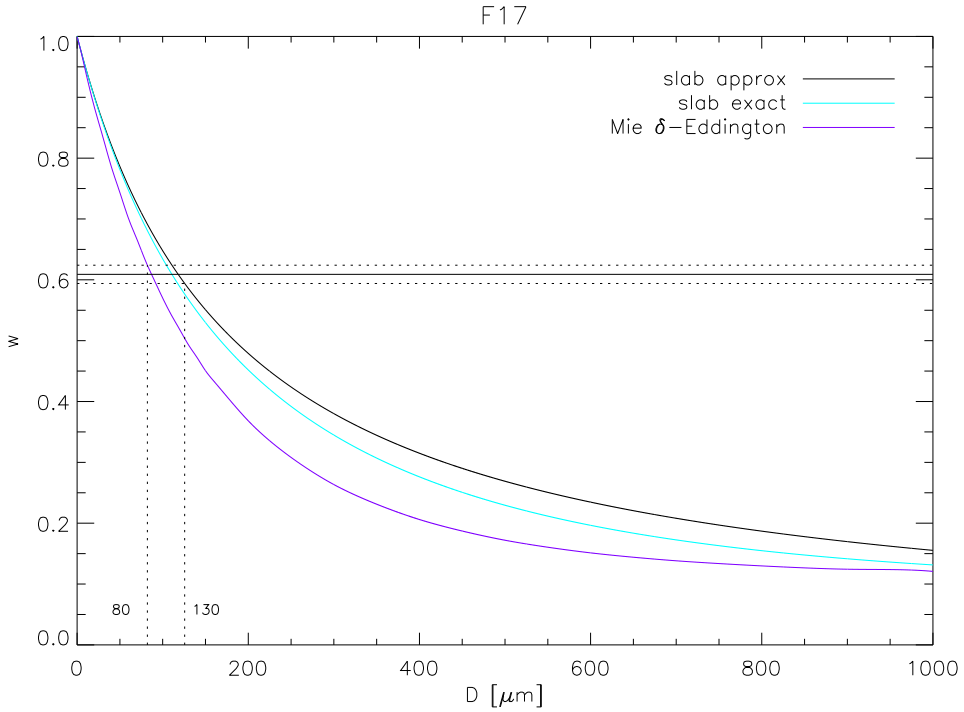

Fig. 7. Approximate and exact Hapke's slab models and Mie-δEddington model of $w(D)$ for amorphous enstatite particles compared with observed single scattering albedo (horizontal line). This select a range of typical grain size.

4. Conclusions

The results of the performed analysis allow us to conclude that the method of modeling the phase curve is very useful in investigating the reflectance behavior of small atmosphereless bodies, giving a good description of the most important properties of the surface scattering regolith layer.

The comparison with more accurate calculations (Spjuth *et al.*, 2009), which take into account the shape of the object, shows that our simplified method is robust and reliable for a preliminary shape-independent analysis.

Acknowledgements. WAC was realised enterely at the University of Padova at the CISAS "G. Colombo" (Center of Studies and Activities for Space), thanks to fundings of ASI (Italian Space Agency) and INAF (National Institute of Astrophysics).

References

Barucci, M. A. *et al.* 2008, A&A, 430, 313
Benner, L. A. M. *et al.* 2008, Icarus, 198, 2, 294
Hapke, B. 1993, Cambridge University Press
Hansen, G. B. 2009, Icarus, 203, 2, 672
Jäger, C. *et al.* 2003, A&A, 408, 193
Joseph, J. H. & Wiscombe W. J. 1976, Journal of the Atmospheric Sciences, 33, 2452
Keller, H. U. Barbieri, C. *et al.* 2010, Science, 327, 5962, 190
Levenberg, K. 1944, The quarterly of applied mathematics, 2, 164
Li, J.-Y. *et al.* 2004, Icarus, 172, 2, 15
Marquardt, D. 1963, SIAM Journal on Applied Mathematics, 11, 431
Sierks, H. 2011, Science, in press
Spjuth, S., 2009, PhD Thesis, Copernicus Publications 2009